

Supporting Information

Enhancement of Electron-donating Character in Alkylated Monopyrrolo- tetrathiafulvalene Derivatives

Kai R. Korsching,^a Hannes Schäfer,^a Josefine Schönborn,^a Arunpatcha Nimthong-Roldán,^b
Matthias Zeller^b and Vladimir A. Azov*^a

^a *University of Bremen, Department of Chemistry, Leobener Str. NW 2C, D-28359 Bremen, Germany; e-mail: vazov@uni-bremen.de, vlazov@gmail.com*

^b *One University Plaza, Youngstown State University, Department of Chemistry, Youngstown, OH 44555-3663, USA*

Table of Contents

Experimental	S2
NMR spectra	S5
HRMS spectra	S10
UV/Vis spectra	S11
Cyclic Voltammetry	S12
Determination of binding constants	S13
Crystal structure of 5 and 8	S16
References	S20

Experimental

General. 5,17-Dibromo-25,26,27,28-tetra-(1-propoxy)calix[4]arene **7**,¹ and monopyrrolo-tetrathiafulvalene derivatives **8b** and **9b**² were prepared as reported previously. Reagent grade chemicals and solvents, including dry dioxane (*Acros*, extra dry, over molecular sieves) and CuI ($\geq 99.5\%$), were used without further purification. All reactions were carried out under an atmosphere of dry N₂. Chemical shifts (δ) are reported in parts per million (ppm) relative to TMS, the residual solvent signals were used as reference: CDCl₃ (7.26 ppm for ¹H, 77.0 ppm for ¹³C) or CD₂Cl₂ (5.32 ppm for ¹H, 53.8 ppm for ¹³C), DMSO-*d*₆ (2.50 ppm for ¹H, 39.5 ppm for ¹³C). ¹H NMR coupling constants (*J*) are reported in Hertz (Hz) and multiplicity is indicated as follows: s (singlet), d (doublet), t (triplet), m (multiplet). High resolution MS-spectra (HRMS) were measured with *Finnigan MAT 95* (EI, 70 eV) and *Thermo Fisher Scientific LTQ Orbitrap* spectrometers (ESI). UV/Vis measurements were performed in a 1 cm path length quartz optical cell. Melting points were determined using a capillary melting point apparatus and are uncorrected. R_f values were determined using 0.2 mm silica gel F-254 aluminum TLC cards, which were inspected under 254 nm UV light. Flash chromatography (FC) was carried out using 230–440 mesh (particle size 36–70 μ m) silica gel.

2-[4,5-Dimethyl-1,3-dithiol-2-yliden]-5-tosyl-[1,3]-dithiolo[4,5-c]pyrrol **2.** Ketone **3** (1.00 g, 3.21 mmol) and thione **4** (0.782 g, 4.82 mmol, 1.5 eq.) were suspended in 15 mL of freshly distilled P(OEt)₃ and heated up to 130 °C upon stirring by setting the reaction flask into the pre-heated oil bath. Two additional portions of thione **4** followed (second portion: 0.521 g, 3.21 mmol, 1 eq.; third portion: 0.261 g, 1.61 mmol, 0.5 eq.) with 15 min intervals. The reaction mixture was then stirred for 3 h, cooled to room temperature, then the solvent was removed using Kugelrohr. The residue was suspended in 50 mL MeOH and stirred overnight. The yellow precipitate was filtered and washed with MeOH (2 \times 30 mL), dried and filtered through a plug of silica (CH₂Cl₂). The fractions with R_f = 0.7–0.8 (CH₂Cl₂), containing the target product **2** and its isomer **5**, have been collected. The mixture was triturated in boiling CH₂Cl₂/cyclohexane (2:1, 2 \times 15 mL) to remove the much better soluble **5**. The solid residue was dried under vacuum to afford the target product as yellow crystalline powder very poorly soluble in most of organic solvents. The best solubility was observed in DMSO. Yield: 0.349 g (0.820 mmol, 26%). M.p. 250–255 °C (decomp.). R_f = 0.72 (CH₂Cl₂), R_f = 0.40 (CH₂Cl₂/cyclohexane, 2:1). ¹H NMR (360 MHz, DMSO-*d*₆, 50 °C): δ 7.79–7.83 (m, 2H), 7.43–7.47 (m, 2H), 7.32 (s, 2H), 2.39 (s, 3H), 1.94 (s, 6H). ¹³C NMR (90 MHz, DMSO-*d*₆, 50 °C): δ 145.5, 134.4, 130.1, 126.53, 126.48, 122.1, 115.4, 112.1, 110.8, 20.8, 13.04. ¹H NMR (200

MHz, CDCl₃): δ 7.68–7.74 (m, 2H), 7.26–7.31 (m, 2H), 6.90 (s, 2H), 2.41 (s, 3H), 1.93 (s, 6H). MS (EI): m/z (%) 425 (60) [M]⁺, 270 (100) [M-Ts]⁺. HRMS (EI): m/z [M]⁺ calcd. for C₁₇H₁₅NO₂S₅⁺: 424.97064; found 424.97118.

11,12-Dimethyl-5-(4-methylbenzenesulfonyl)-2,8,10,13-tetrathia-5-

azatricyclo[7.4.0.0^{3,7}]trideca-1(9),3,6,11-tetraen 5. The liquid phase after the trituration was evaporated to dryness, and compound **5** was additionally purified by FC (CH₂Cl₂/cyclohexane, 2:1), affording colorless crystalline powder. X-ray quality crystals were obtained by slow evaporation of CH₂Cl₂/cyclohexane solution. Yield: 0.132 g (0.310 mmol, 10%). M.p. 240–242 °C. R_f = 0.74 (CH₂Cl₂), R_f = 0.44 (CH₂Cl₂/cyclohexane, 2:1). ¹H NMR (360 MHz, CDCl₃): δ 7.72–7.75 (m, 2H), 7.31–7.33 (m, 2H), 6.94 (s, 2H), 2.43 (s, 3H), 1.99 (s, 6H). ¹³C NMR (90 MHz, CDCl₃): δ 145.8, 135.1, 130.3, 130.1, 127.1, 122.5, 120.9, 116.2, 21.7, 20.3. MS (EI): m/z (%) 425 (100) [M]⁺, 270 (90) [M-Ts]⁺. HRMS (EI): m/z [M]⁺ calcd. for C₁₇H₁₅NO₂S₅⁺: 424.97046; found 424.97063.

2-[4,5-Dimethyl-1,3-dithiol-2-yliden]-[1,3]-dithiolo[4,5-c]pyrrol 1. *N*-Tosyl MPTTF derivative **2** (0.229 g, 0.537 mmol) was suspended in 20 mL of abs. MeOH/THF (1:1) mixture, 1.4 mL of 5.8 M NaOMe/MeOH soln were added to the reaction mixture, which was then degassed using the *freeze-pump-thaw* method. After that the reaction mixture was refluxed for 30 min, cooled to room temperature, and concentrated to dryness. To the residue 20 mL of H₂O/MeOH (1:1) mixture were added, precipitate formed was filtered, dried, and then purified by FC (silica, CH₂Cl₂ + 1% Et₃N). The target product **1** was isolated as orange crystals. Yield: 0.131 g (0.484 mmol, 90%). M.p. 189–190 °C (decomp.). R_f = 0.65 (CH₂Cl₂). ¹H NMR (360 MHz, CDCl₃): δ 8.13 (bs, 2H), 6.58 (d, J = 2.6 Hz, 2H), 1.95 (b, 6H). ¹³C NMR (90 MHz, CDCl₃): δ 122.3, 120.6, 114.9, 109.5, 13.7. MS (EI): m/z (%) 271 (100) [M]⁺, 174 (25) [M-C₄H₃NS]⁺, 141 (30) [M-C₅H₆S₂]⁺. HRMS (EI): m/z [M]⁺ calcd. for C₁₀H₉NS₄⁺: 270.96179; found 270.96105. CV (*vs.* SCE, CH₂Cl₂): E_{1/2}^{ox1} = 0.18 V.

Copper-catalyzed N-arylation reaction of monopyrrolo-tetrathiafulvalenes, general procedure. A heavy walled Schlenk tube with a wide bore Teflon screw stopcock was charged with MPTTF derivative **1**, CuI, K₃PO₄, (\pm)-*trans*-1,2-diaminocyclohexane and an aromatic bromide, then absolute dioxane was added via syringe. The reaction mixture was degassed by three freeze-pump-thaw cycles, the vessel was filled with nitrogen, tightly sealed and stirred at 110 °C. The reaction was complete for 48–60 h. The solvent was removed under reduced pressure directly from the Schlenk tube, the residue was dissolved in CH₂Cl₂ and filtered through a plug of celite, and evaporated to dryness. The crude products were triturated with *n*-hexane to remove the unreacted aromatic starting material and then purified by flash chromatography on silica gel to afford pure *N*-arylated MPTTFs.

2-[4,5-Dimethyl-1,3-dithiol-2-ylidene]-5-(4-methoxyphenyl)-5H-1,3-dithiolo[4,5-c]pyrrole 8a. Prepared from **1** (0.0156 g, 0.0575 mmol), CuI (0.011 g, 0.0575 mmol), K₃PO₄ (0.0976 g, 0.0459 mmol), *trans*-diaminocyclohexane (11 μL, 0.246 mmol) and 4-bromoanisole **6** (0.043 g, 0.230 mmol) in 3 mL of dry dioxane by heating for 48 h at 110 °C. The product was purified by flash chromatography (CH₂Cl₂/cyclohexane, 2:1) to afford yellow crystalline powder. Compound **8a** afforded X-ray quality crystals were obtained by slow evaporation of an NMR sample (CD₂Cl₂). Yield: 18.5 mg (0.049 mmol, 85%). M.p. 214–216 °C (decomp.). R_f = 0.40 (CH₂Cl₂/cyclohexane, 1:1). ¹H NMR (360 MHz, CD₂Cl₂): δ 7.24–7.28 (m, 2H), 6.92–6.97 (m, 2H), 6.82 (s, 2H), 3.81 (s, 3H), 1.96 (s, 6H). ¹³C NMR (90 MHz, CD₂Cl₂): δ 158.3, 134.3, 129.9, 122.8, 122.0, 115.0, 113.9, 111.6, 55.9, 13.8. UV/Vis (CH₂Cl₂): λ_{max} (ε) 319 nm (23000 L·mol⁻¹·cm⁻¹), 450 (350). MS (EI): *m/z* (%) 377 (100) [M]⁺. HRMS (EI): *m/z* [M]⁺ calcd. for C₁₇H₁₅NOS₄⁺: 377.00365; found 377.00321. CV (*vs.* SCE, CH₂Cl₂): E_{1/2}^{ox1} = 0.41 V, E_{1/2}^{ox2} = 0.84 V.

5,17-Bis[2-[4,5-dimethyl-1,3-dithiol-2-ylidene]-5H-1,3-dithiolo[4,5-c]pyrrol-5-yl]-25,26,27,28-tetra-(1-propoxy)calix[4]arene 9a. Prepared from **1** (0.100 g, 0.368 mmol), CuI (0.028 g, 0.147 mmol), K₃PO₄ (0.250 g, 1.18 mmol), *trans*-diaminocyclohexane (25 μL, 0.221 mmol) and calixarene **7** (0.110 g, 0.147 mmol) in 10 mL of dry dioxane by heating for 60 h at 110 °C. The product was purified by flash chromatography (CH₂Cl₂/cyclohexane, 1:2) to afford bright yellow crystals. Mono-substituted calix[4]arene derivative was separated as a major by-product with a slightly lower R_f value. Yield: 75 mg (0.066 mmol, 45%). M.p. 209–211 °C (decomp.). R_f = 0.30 (CH₂Cl₂/cyclohexane, 1:2). ¹H NMR (360 MHz, CD₂Cl₂): δ 7.02–7.04 (m, 4H), 6.85–6.90 (m, 2H), 6.20 (s, 4H), 6.04 (s, 4H), 4.48 (d, ²J = 13.3 Hz, 4H), 3.99–4.04 (m, 4H), 3.72 (t, ³J = 7.2 Hz, 4H), 3.18 (d, ²J = 13.3, 4H), 1.90–2.03 (m, 8H), 1.89 (s, 12H), 1.09 (t, ³J = 7.2 Hz, 6H), 0.94 (t, ³J = 7.2 Hz, 6H). ¹³C NMR (90 MHz, CD₂Cl₂): δ 157.8, 154.2, 136.4, 135.6, 135.1, 129.2, 122.7, 122.6, 122.0, 119.6, 110.4, 77.6, 77.1, 31.3, 23.8, 23.4, 13.7, 10.9, 10.1. UV/Vis (CH₂Cl₂): λ_{max} (ε) 309 nm (38000 L·mol⁻¹·cm⁻¹), 452 (700). HRMS (ESI⁺): *m/z* [M]⁺ calcd. for C₆₀H₆₂N₂O₄S₈⁺: 1130.24698; found 1130.24805. CV (*vs.* SCE, CH₂Cl₂): E_{1/2}^{ox1.1} = 0.17 V, E_{1/2}^{ox1.2} = 0.33 V, E_{1/2}^{ox2} = 0.80 V.

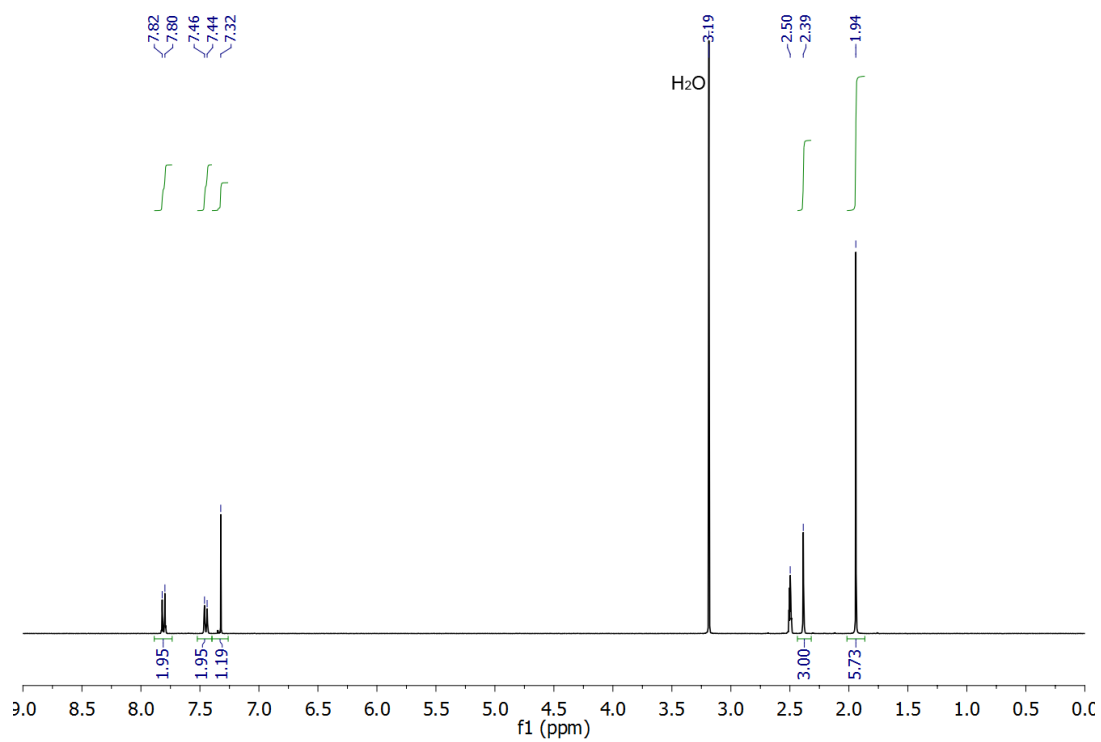


Figure S1a. ^1H NMR spectrum of compound **2** (360 MHz, DMSO- d_6 , 50 °C).

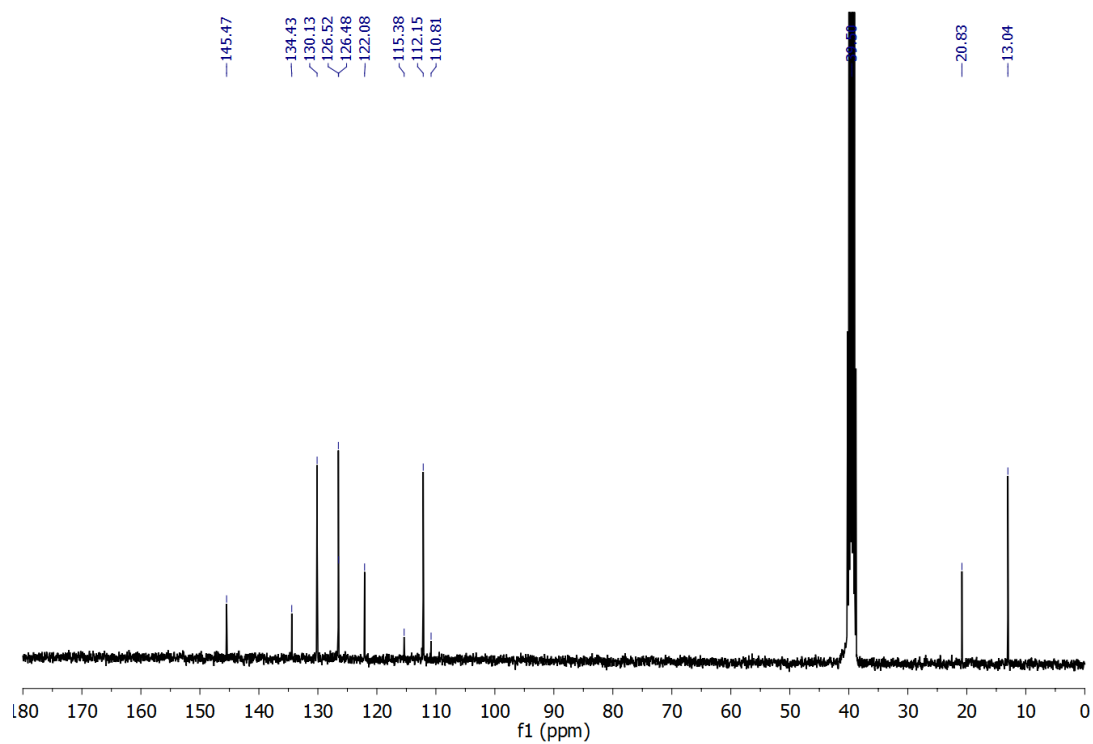


Figure S1b. ^{13}C NMR spectrum of compound **2** (90 MHz, DMSO- d_6 , 50 °C).

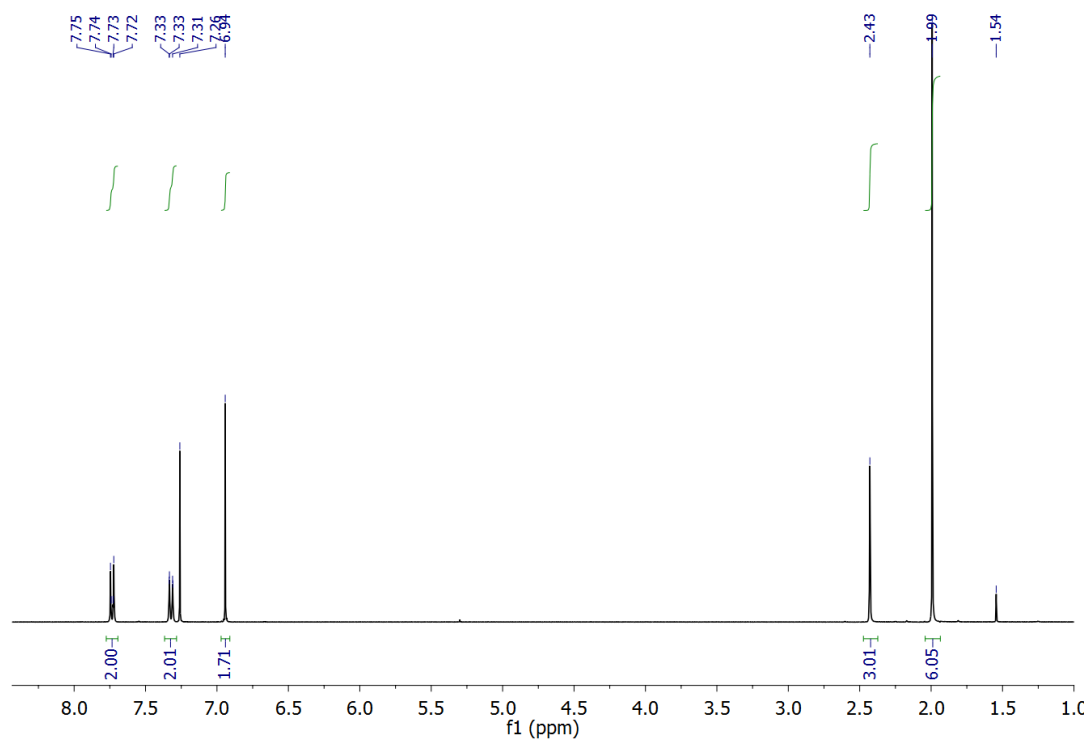


Figure S2a. ^1H NMR spectrum of compound **5** (360 MHz, CDCl_3).

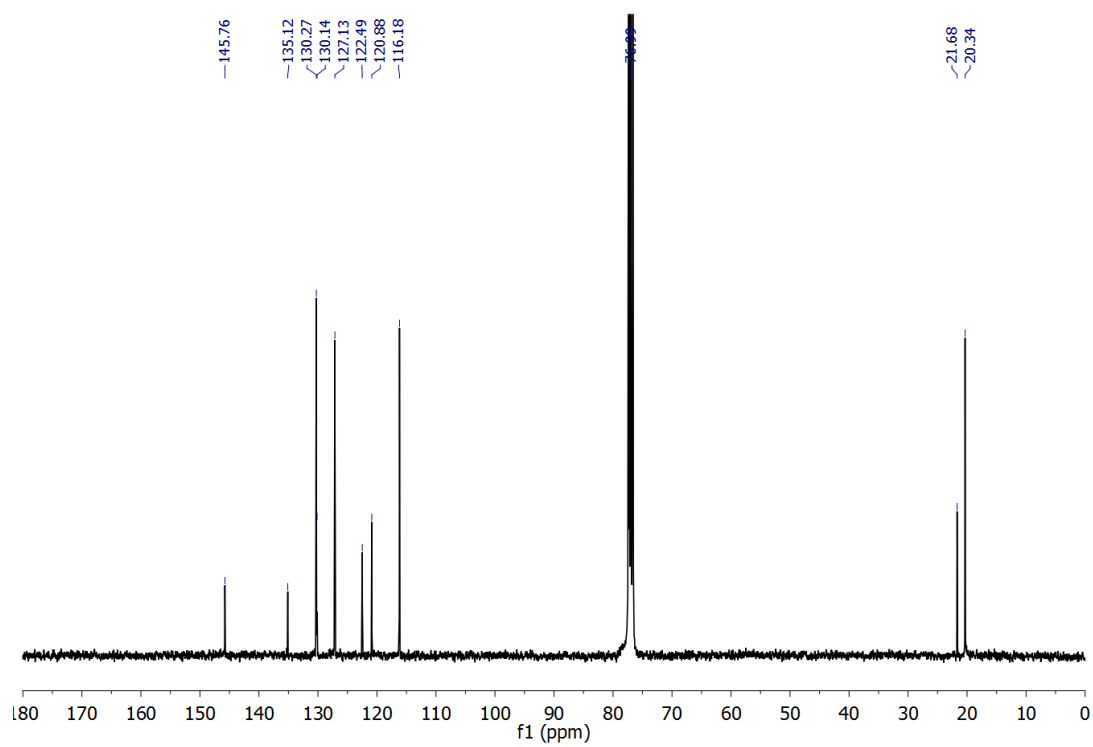


Figure S2b. ^{13}C NMR spectrum of compound **5** (90 MHz, CDCl_3).

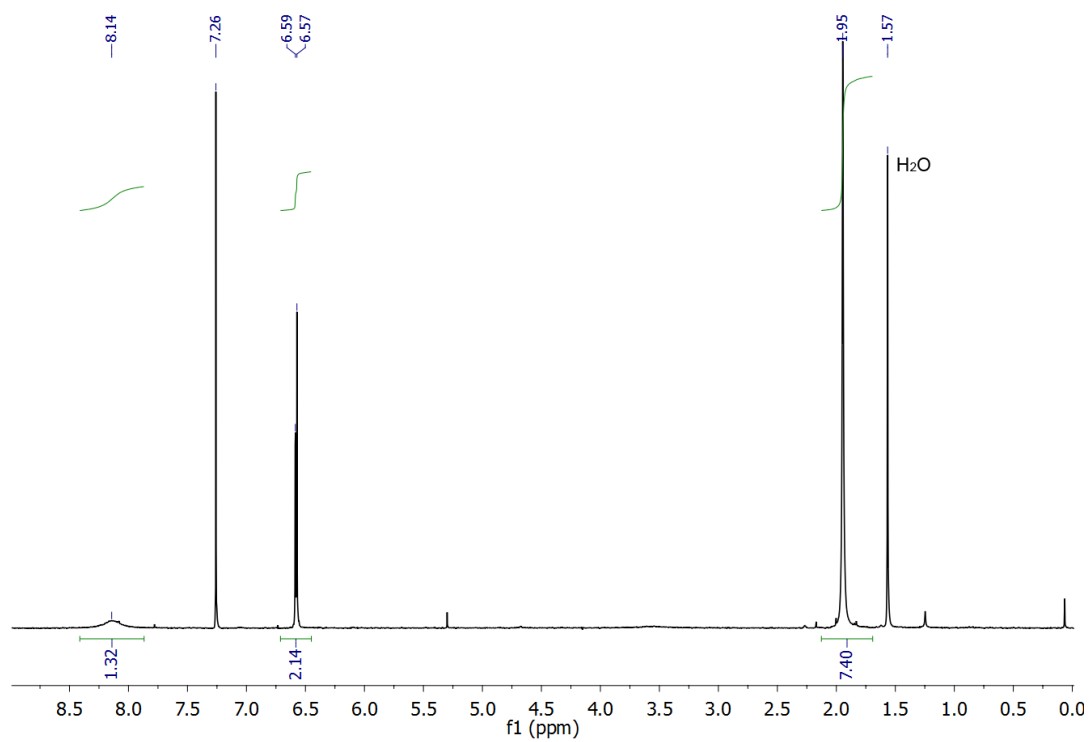


Figure S3a. ¹H NMR spectrum of compound **1** (360 MHz, CDCl₃).

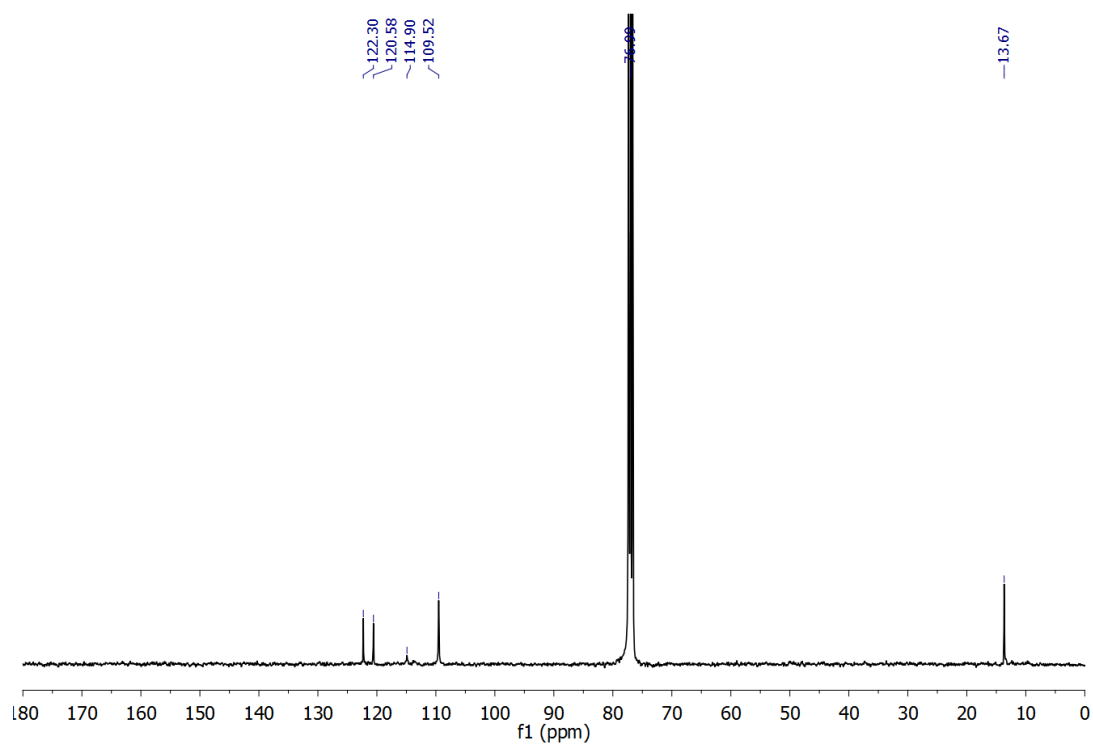


Figure S3b. ¹³C NMR spectrum of compound **1** (90 MHz, CD₂Cl₂).

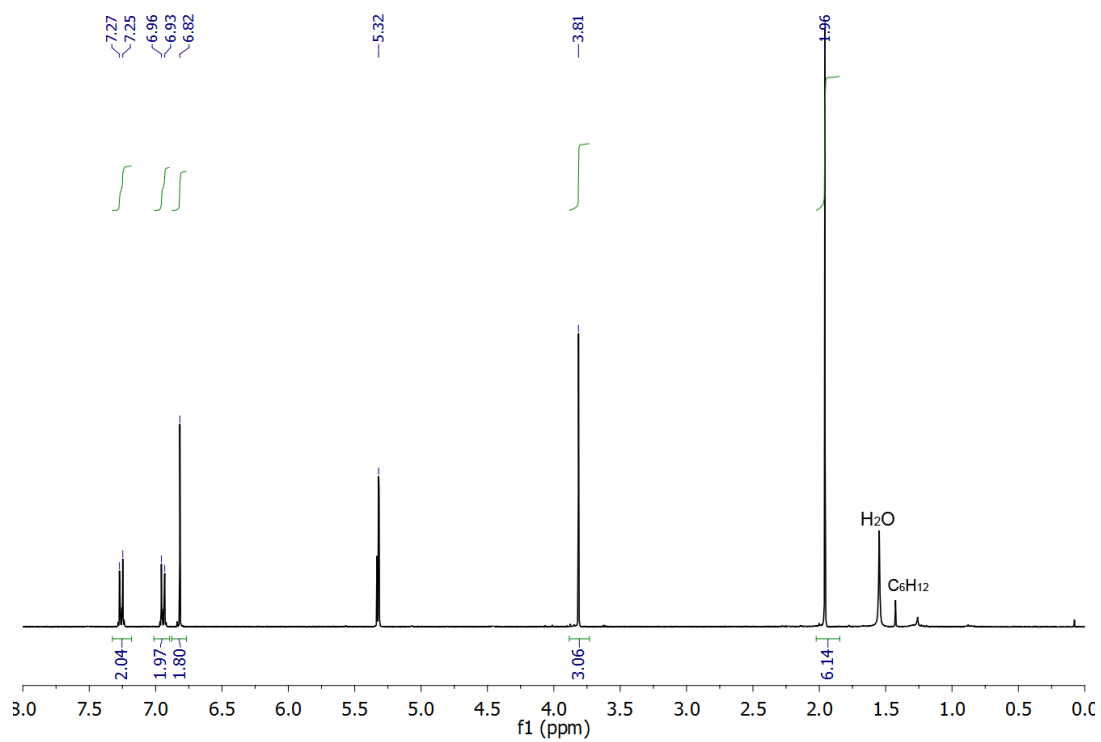


Figure S4a. ^1H NMR spectrum of compound **8a** (360 MHz, CD_2Cl_2).

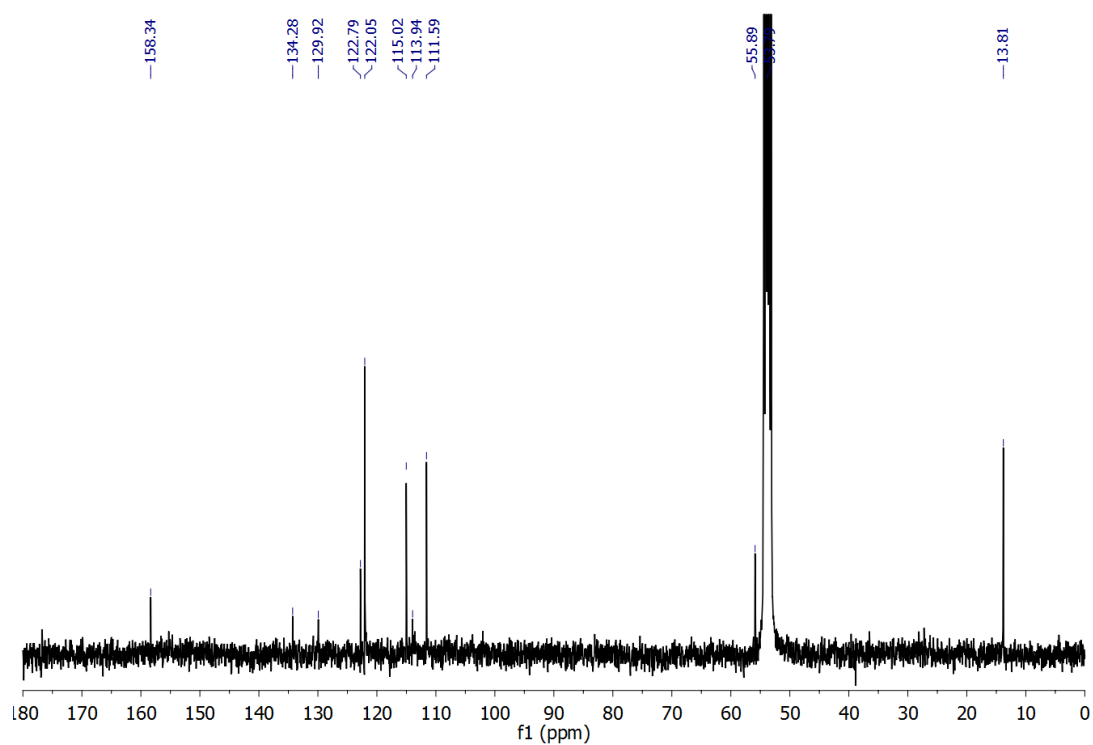


Figure S4b. ^{13}C NMR spectrum of compound **8a** (90 MHz, CD_2Cl_2).

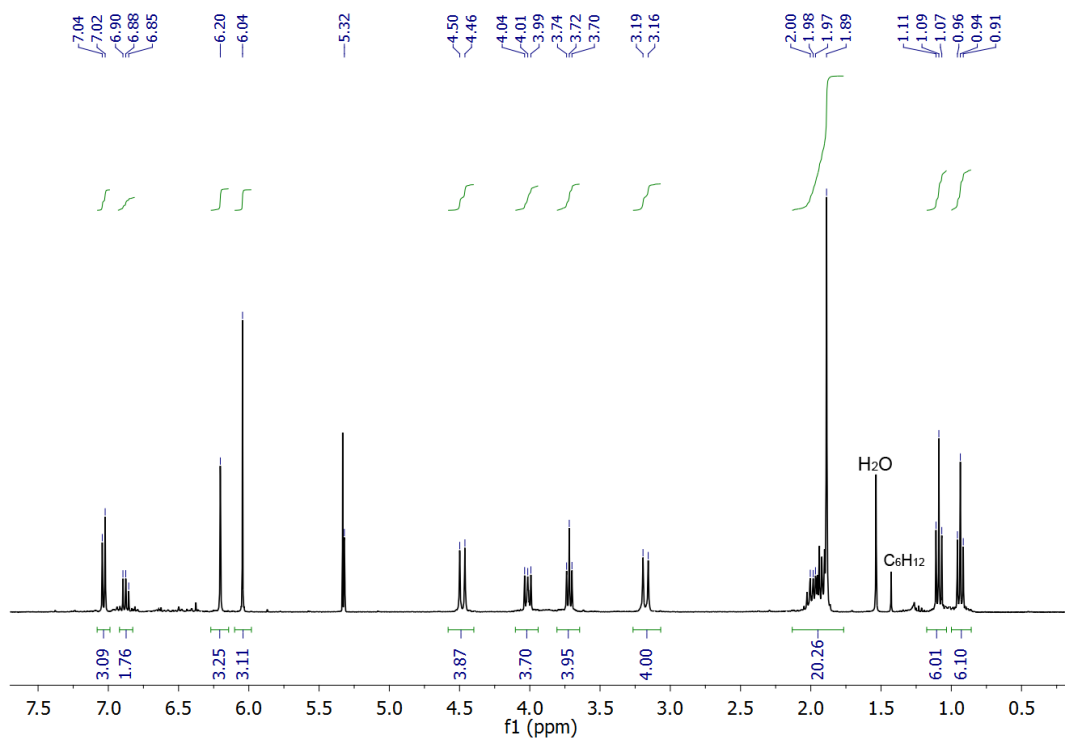


Figure S5a. ¹H NMR spectrum of compound **9a** (360 MHz, CD₂Cl₂).

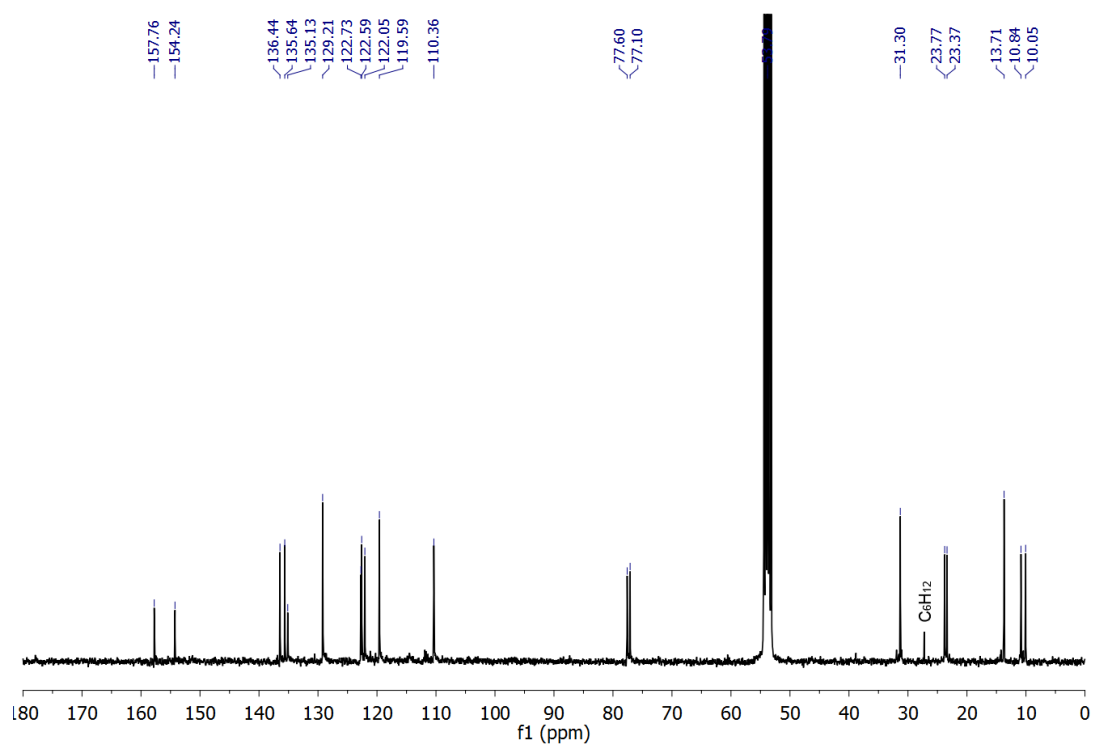


Figure S5b. ¹³C NMR spectrum of compound **9a** (90 MHz, CD₂Cl₂).

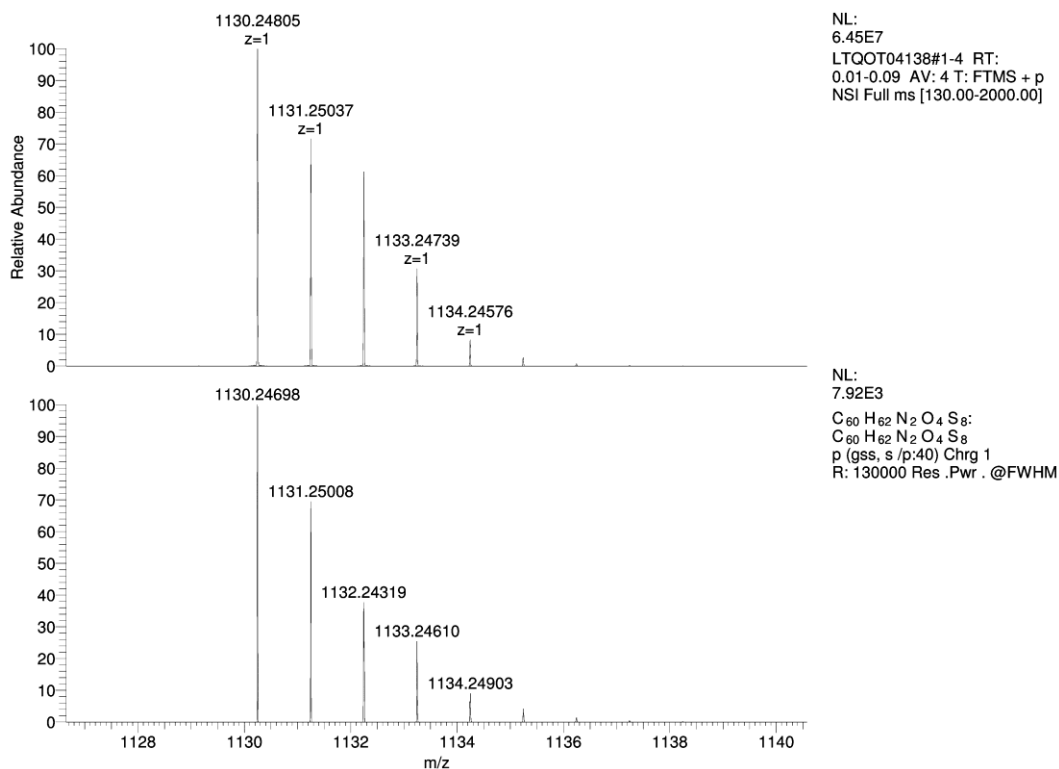


Figure S6. HR-ESI-MS spectrum of compound **9a** showing the high-resolution isotope pattern of the M^+ ion, observed (above) and simulated (below).

UV/Vis Spectra

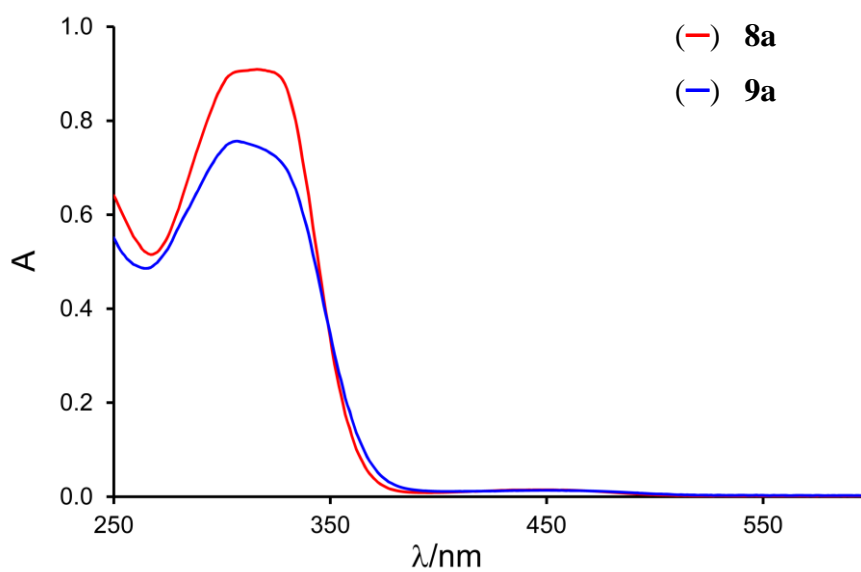


Figure S7. UV/Vis spectra of compounds **8a** (red), **9a** (blue). CH_2Cl_2 , $c = 4 \times 10^{-5}$ M (**8a**) or $c = 2 \times 10^{-5}$ M (**9a**).

Cyclic voltammetry

Cyclic Voltammetry (CV) was performed using a computer controlled *HEKA PG390* potentiostat in a three-electrode single-compartment cell (2.5 ml) with a platinum disk working electrode (diameter of 1.5 mm) and a platinum wire used as a counter electrode. A non-aqueous Ag/Ag⁺ secondary electrode, containing 0.1 M Bu₄NClO₄ (TBAP) + 0.01 M AgNO₃ in MeCN, was used as the reference electrode. CV samples were dissolved to a concentration of 1×10⁻³ M in dry degassed CH₂Cl₂ containing 0.1 M TBAP as supporting electrolyte. Ferrocene (Fc) was used as an electrochemical reference³ with the potential $E_{1/2}^{ox} = 0.48$ V vs. saturated calomel electrode (SCE) for the Fc/Fc⁺ couple in 0.1 M TBAP/CH₂Cl₂.⁴ Thus, a CV scan of 1×10⁻³ M Fc solution was taken after each CV measurement for calibration purposes. Then the values of oxidation potentials were referenced to the Fc/Fc⁺ couple, recalculated and reported vs. SCE.

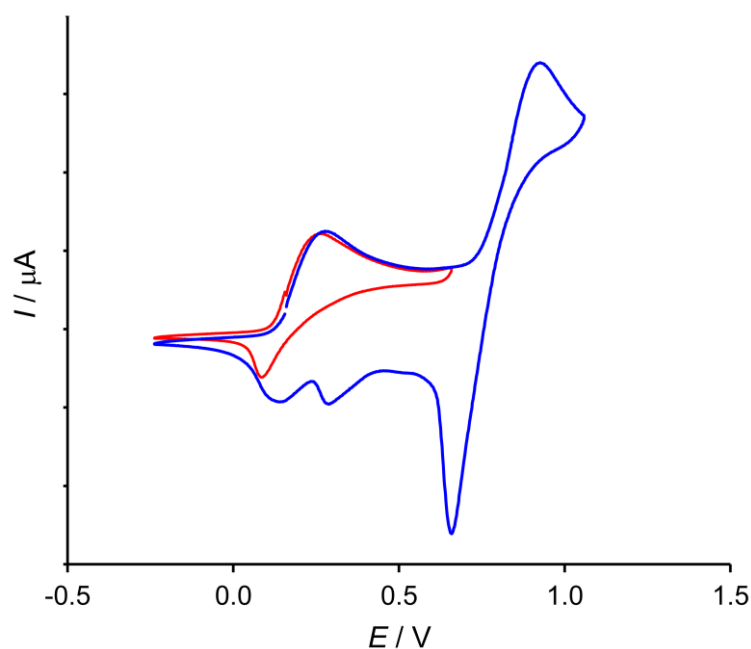


Figure S8. Cyclic voltammograms of compound **1** recorded within two different scan intervals (CH₂Cl₂/0.1 M Bu₄NClO₄, 100 mV/s).

Binding titration experiments

Determination of binding constants by UV/vis dilution method

The dilution experiments were carried out in a quartz cell with 1 cm path length at 23 °C in CH₂Cl₂. For the dilution method,⁵ the host concentration [H]⁰ and guest concentrations [G]⁰ are kept equimolar from the start, and the solution is subsequently stepwise diluted with solvent before each measurement.

The following equation applies to the dilution method with regards to the concentration of a host-guest complex c , the measured absorption A , binding constant K_a , extinction coefficient of the host-guest complex ε , and path length d :

$$\frac{c}{A} = \left(\frac{1}{K_a \cdot \varepsilon \cdot d}\right)^{1/2} \cdot \frac{1}{A^{1/2}} + \frac{1}{\varepsilon \cdot d} \quad (1)$$

Based on equation (1), $\frac{c}{A}$ is plotted vs $\frac{1}{A^{1/2}}$, which results in a straight line. From the values for the slope of the line $\alpha = \left(\frac{1}{K_a \cdot \varepsilon \cdot d}\right)^{1/2}$ and its y-intercept $y_0 = \frac{1}{\varepsilon \cdot d}$, the values for the binding constant K_a and the extinction coefficient of the complex ε can be calculated as:

$$K_a = \frac{y_0}{\alpha^2} \quad \text{and} \quad \varepsilon = \frac{1}{y_0 \cdot d}$$

The estimated error on K_a is $< \pm 15\%$. The method was validated using binding titration between [CBPQT⁴⁺] \cdot 4[PF₆⁻] and non-substituted tetrathiafulvalene in acetone, affording the binding constant K_a within 10% error from the reported values.⁵

Titration experiments were performed by removal of 0.1 mL of the original 0.8 mL host-guest solution and dilution of the remaining 0.7 mL of solution by 0.1 mL of pure CH₂Cl₂. For **9a**, dilution UV/vis experiments were started at concentrations [9] = [TCNQ] $< 1.5 \times 10^{-4}$ M, since above this concentration plot non-linearity was observed, likely due to the aggregation of host-guest complexes. For **9b**, TCNQ binding constant, redetermined using dilution method, was found to be much higher than previously reported one² due to the very slow precipitation of the host-guest complex at concentrations higher than 5.00×10^{-4} M.

Plots

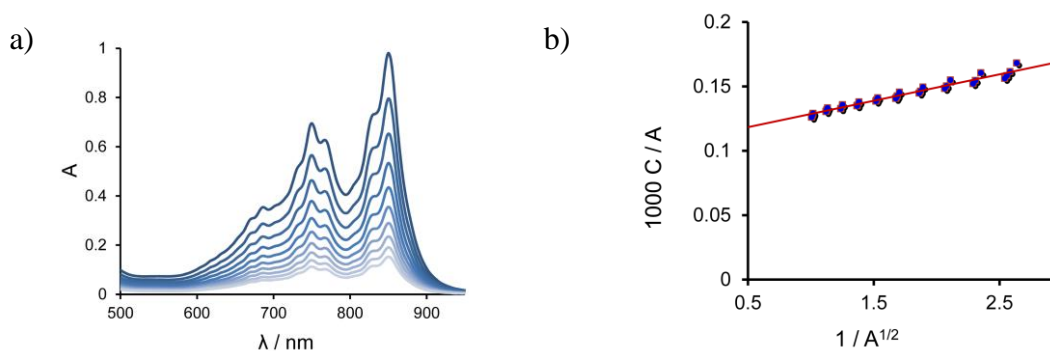


Figure S9. (a) UV/vis dilution of **9a** with TCNQ (CH_2Cl_2). The absorbance A was measured at concentrations $C_{\text{host}} = C_{\text{guest}}$ varied in the range $1.25 \times 10^{-4} \text{ M} - 2.42 \times 10^{-5} \text{ M}$. (b) A linear plot of c/A against $1/A^{1/2}$ for a 1:1 mixture of derivative **9a** and TCNQ (CH_2Cl_2).

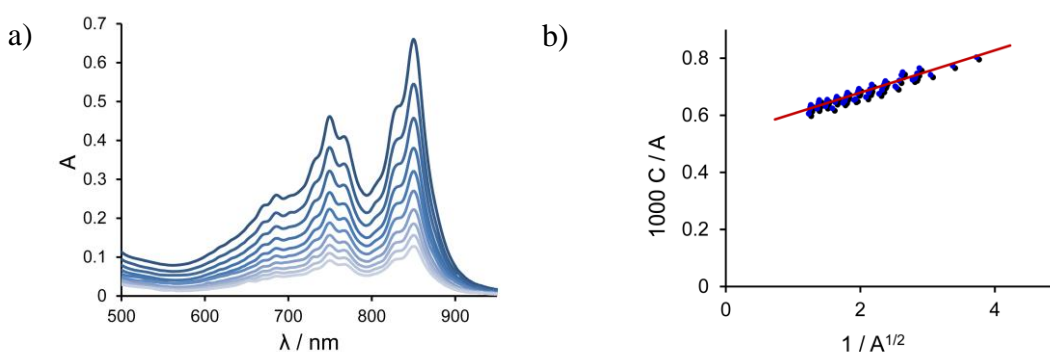


Figure S10. (a) UV/vis dilution of **9b** with TCNQ (CH_2Cl_2). The absorbance A was measured at concentrations $C_{\text{host}} = C_{\text{guest}}$ varied in the range $4.00 \times 10^{-4} \text{ M} - 5.8 \times 10^{-5} \text{ M}$. (b) A linear plot of c/A against $1/A^{1/2}$ for a 1:1 mixture of derivative **9b** and TCNQ (CH_2Cl_2).

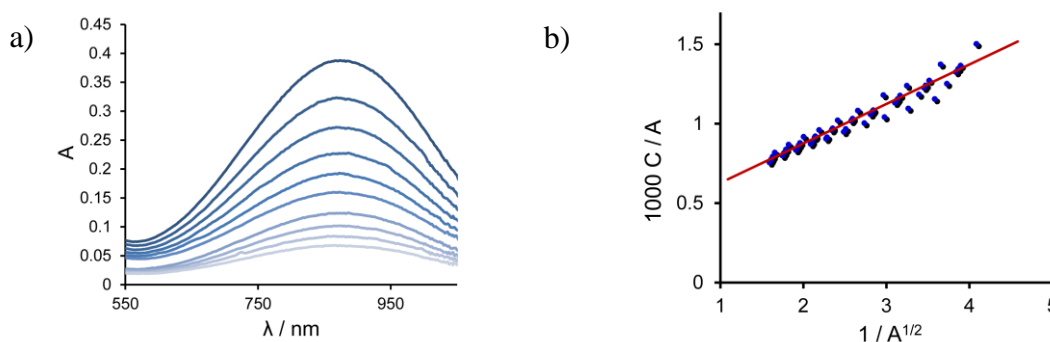


Figure S11. (a) UV/vis titration of **8a** with CBPQT^{4+} (Me_2CO). The absorbance A was measured at concentrations $C_{\text{host}} = C_{\text{guest}}$ varied in the range $3.00 \times 10^{-4} \text{ M} - 9.02 \times 10^{-5} \text{ M}$. (b) A linear plot of c/A against $1/A^{1/2}$ for a 1:1 mixture of derivative **8a** and CBPQT^{4+} (Me_2CO).

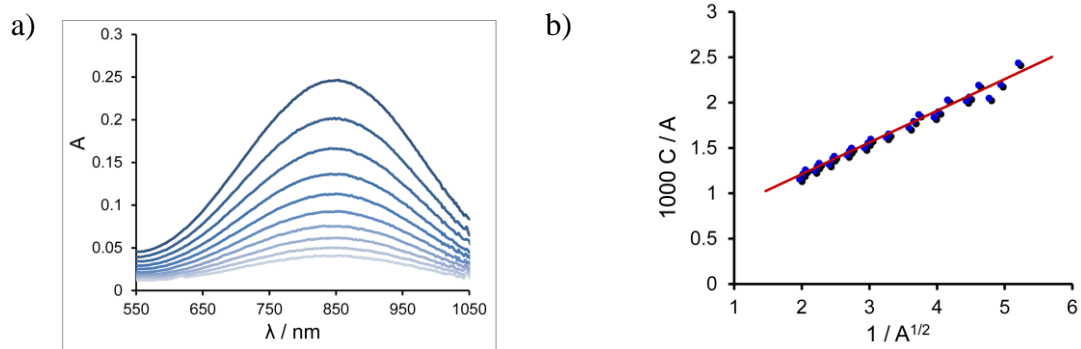


Figure S12. (a) UV/vis dilution of **8b** with CBPQT⁴⁺ (Me₂CO). The absorbance *A* was measured at concentrations $C_{host} = C_{guest}$ varied in the range 3.00×10^{-4} M – 9.02×10^{-5} M. (b) A linear plot of c/A against $1/A^{1/2}$ for a 1:1 mixture of derivative **8b** and CBPQT⁴⁺ (Me₂CO).

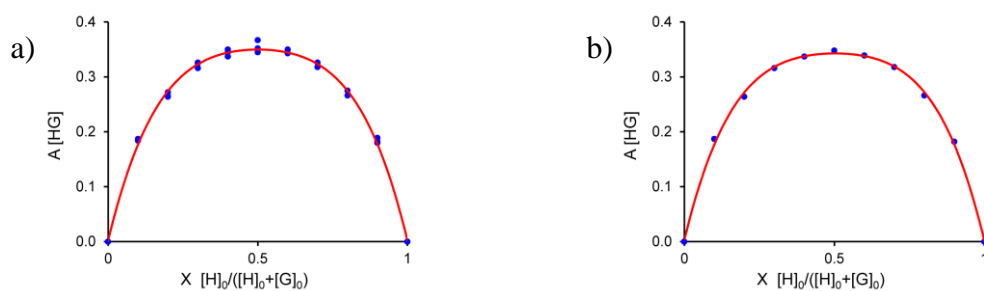


Figure S13. Job plots for the binding of TCNQ with (a) **9a** ($[H]_0 + [G]_0 = 1.0 \times 10^{-4}$ M) and (b) **9b** ($[H]_0 + [G]_0 = 3.3 \times 10^{-4}$ M) in CH₂Cl₂.

X-Ray Crystal Structure Determination

Diffraction data were collected on *Bruker AXS SMART APEX (5)* or *AXS APEXII (8a)* CCD diffractometers at 100 K using monochromatic Mo K α radiation with the omega and phi scan techniques. Data were collected, unit cells determined, and the data integrated and corrected for absorption and other systematic errors using the *Apex2* suite of programs.⁶ The space groups were assigned and the structures were solved by direct methods using the *SHELXTL* suite of programs⁷ and refined by full matrix least squares against F^2 with all reflections using *Shelxl2013* or *Shelxl2014*.⁸ H-atoms attached to carbon atoms were positioned geometrically and constrained to ride on their parent atoms, with carbon hydrogen bond distances of 0.95 and 0.98 Å for aromatic C-H and CH₃ moieties, respectively. U_{iso}(H) values were set to a multiple of U_{eq}(C) with 1.5 for CH₃ and 1.2 for CH units, respectively.

For **5**, methyl hydrogen atoms at C7 were refined as disordered over two positions separated by a 60° rotation. Occupancies refined to 0.67(2) and 0.33(2). Reflection 0 0 1 was affected by the beam stop and was omitted from the refinement.

For **8a**, reflections 1 -2 1 and 0 1 0 were affected by the beam stop and were omitted from the refinement.

X-ray crystallographic data and refinement details are summarized in Table S1.

Complete crystallographic data, in CIF format, have been deposited with the Cambridge Crystallographic Data Centre. These data format can be obtained free of charge from the Cambridge Crystallographic Data Centre via www.ccdc.cam.ac.uk/data_request/cif on quoting the deposit numbers CCDC 1415145 and CCDC 1415146 for **5** and **8a**, respectively.

Table S1. Crystal data and structure refinement for compounds **5** and **8a**.

Crystal data		
Compound	5	8a
Chemical formula	C ₁₇ H ₁₅ NO ₂ S ₅	C ₁₇ H ₁₅ NOS ₄
M_r	425.60	377.54
Crystal system, space group	Triclinic, $P\bar{1}$	Triclinic, $P\bar{1}$
Temperature (K)	100	100
a, b, c (Å)	8.9673 (14), 9.3214 (15), 11.9354 (19)	7.8445 (19), 8.762 (2), 12.265 (3)
α, β, γ (°)	107.566 (2), 103.414 (2), 92.688 (2)	86.427 (3), 81.337 (3), 81.142 (3)
V (Å ³)	917.8 (3)	822.8 (3)
Z	2	2
Radiation type	Mo $K\alpha$	Mo $K\alpha$
μ (mm ⁻¹)	0.64	0.58
Crystal size (mm)	0.55 × 0.52 × 0.39	0.52 × 0.46 × 0.34
Data collection		
Diffractometer	Bruker AXS Smart Apex CCD Diffractometer	Bruker AXS APEXII CCD diffractometer
Absorption correction	Multi-scan, SADABS, Bruker Apex2	Multi-scan, SADABS, Bruker Apex2
T_{\min}, T_{\max}	0.653, 0.746	0.654, 0.746
No. of measured, independent and observed [$I > 2\sigma(I)$] reflections	10464, 5416, 5133	20343, 5245, 4731
R_{int}	0.026	0.026
$(\sin \theta/\lambda)_{\text{max}}$ (Å ⁻¹)	0.732	0.751
Refinement		
$R[F^2 > 2\sigma(F^2)], wR(F^2), S$	0.029, 0.083, 1.02	0.029, 0.085, 1.04
No. of reflections	5416	5245
No. of parameters	230	211
H-atom treatment	H-atom parameters constrained	H-atom parameters constrained
$\Delta\rho_{\text{max}}, \Delta\rho_{\text{min}}$ (e Å ⁻³)	0.53, -0.33	0.51, -0.29

Table S2. Hydrogen-bond geometry (Å, °) for compound **5**.

<i>D</i> —H··· <i>A</i>	<i>D</i> —H	H··· <i>A</i>	<i>D</i> ··· <i>A</i>	<i>D</i> —H··· <i>A</i>
C2—H2···S5 ⁱ	0.95	2.9861 (4)	3.6942 (4)	132.431 (5)
C3—H3···S3 ⁱⁱ	0.95	2.9233 (12)	3.6771 (12)	137.16 (2)
C6—H6···S4 ⁱⁱⁱ	0.95	2.8672 (4)	3.8161 (14)	176.8873 (5)
C8—H8···S2 ⁱⁱ	0.95	3.0610 (4)	4.0103 (5)	177.5644 (3)
C15—H15···O2 ^{iv}	0.95	2.5817 (3)	3.5015 (3)	163.0555 (16)
C16—H16A···O2 ^v	0.98	2.9086 (3)	3.5290 (4)	122.148 (9)
C17—H17A···O1 ^v	0.98	2.8243 (4)	3.5024 (5)	126.975 (9)

Symmetry code: (i) $x, 1+y, +z$; (ii) $-x, 1-y, 1-z$; (iii) $-x, -y, -z$; (iv) $-1-x, -y, -z$; (v) $-x, -y, 1-z$.

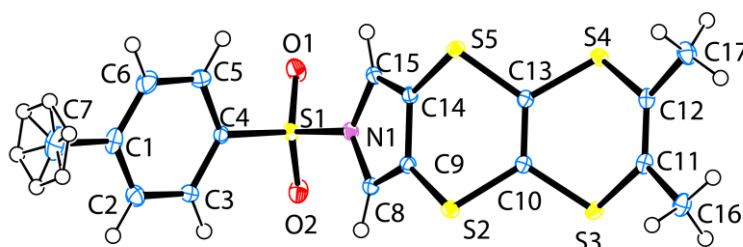


Figure S14. ORTEP plot of **5**. The H-atoms of the methyl group C7 exhibit disorder by a 60 degree rotation with occupancy rates of 0.67(2) and 0.33(2). Thermal ellipsoids are shown at the 50% probability level. Hydrogen atoms are shown as spheres of arbitrary radius.

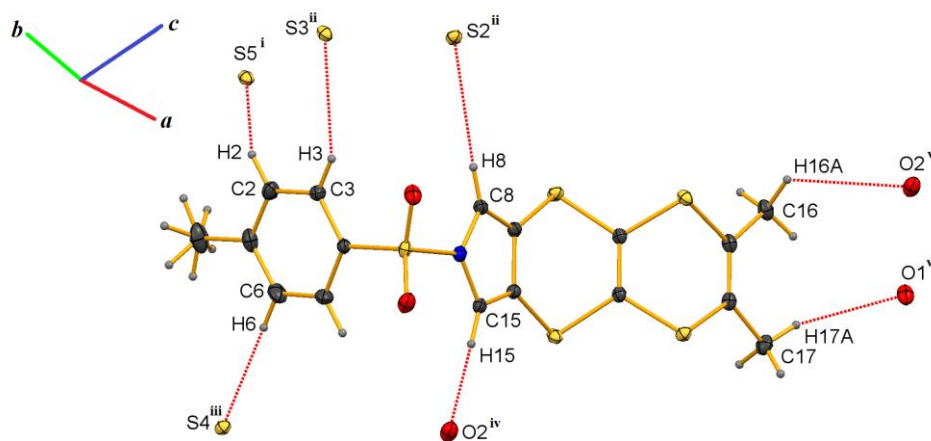


Figure S15. Plot of **5** depicting intramolecular H-bonds and intermolecular interactions with distances shorter than the Van der Waals contacts.

Table S2. Hydrogen-bond geometry (Å, °) for compound **8a**.

<i>D</i> —H··· <i>A</i>	<i>D</i> —H	H··· <i>A</i>	<i>D</i> ··· <i>A</i>	<i>D</i> —H··· <i>A</i>
C6—H6A···S4 ⁱ	0.98	2.94	3.8720 (13)	158.3
C7—H7···S3 ⁱⁱ	0.95	2.96	3.7193 (13)	137.9
C15—H15···S2 ⁱⁱⁱ	0.95	2.90	3.5918 (13)	130.8
C17—H17A···N1 ^{iv}	0.98	2.66	3.5758 (15)	155.2
C17—H17C···O1 ^v	0.98	2.54	3.4226 (14)	149.1

Symmetry code: (i) $x-1, y, z$; (ii) $-x, -y+2, -z+1$; (iii) $-x, -y+2, -z$; (iv) $x+1, y, z$; (v) $-x+2, -y+3, -z$.

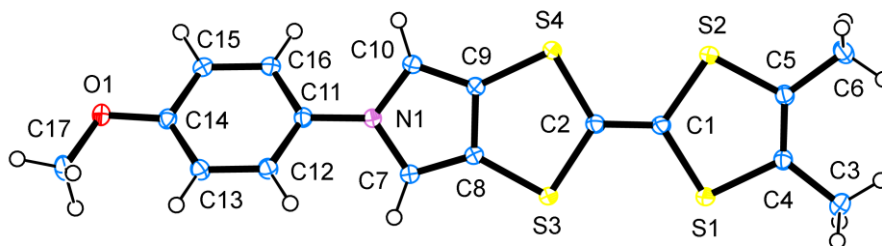


Figure S16. ORTEP plot of **8a**. Thermal ellipsoids are shown at the 50% probability level. Hydrogen atoms are shown as spheres of arbitrary radius.

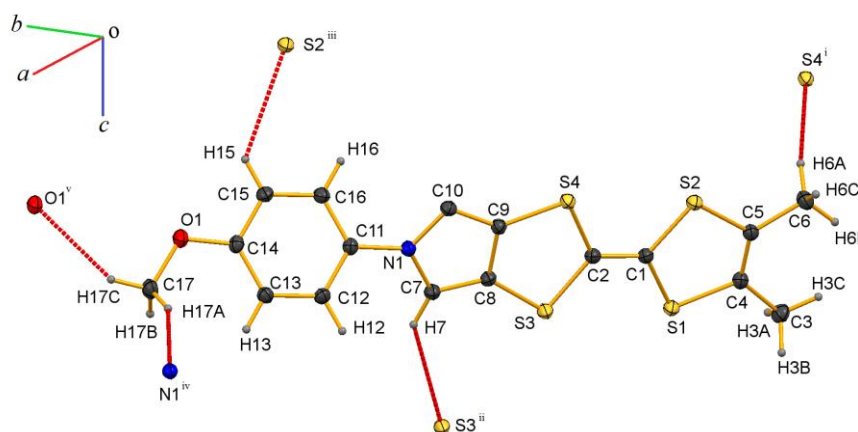


Figure S17. Plot of **8a** depicting intramolecular H-bonds and intermolecular interactions with distances shorter than the Van der Waals contacts.

References

1. A. Casnati, M. Fochi, P. Minari, A. Pochini, M. Reggiani, R. Ungaro and D. Reinhoudt, *Gazz. Chim. Ital.*, 1996, **126**, 99–106.
2. M. H. Düker, H. Schäfer, M. Zeller and V. A. Azov, *J. Org. Chem.*, 2013, **78**, 4905–4912.
3. (a) G. Gritzner and J. Kuta, *Pure Appl. Chem.*, 1984, **56**, 461–466; (b) V. V. Pavlishchuk and A. W. Addison, *Inorg. Chim. Acta*, 2000, **298**, 97–102; (c) N. G. Connely and W. E. Geiger, *Chem. Rev.*, 1996, **96**, 877–910.
4. (a) D. Chang, T. Malinski, A. Ulman and K. M. Kadish, *Inorg. Chem.*, 1984, **23**, 817–824; (b) S. V. Rosokha and J. K. Kochi, *J. Am. Chem. Soc.*, 2007, **129**, 3683–3697.
5. M. B. Nielsen, J. O. Jeppesen, J. Lau, C. Lomholt, D. Damgaard, J. P. Jacobsen, J. Becher and J. F. Stoddart, *J. Org. Chem.*, 2001, **66**, 3559–3563.
6. *Apex2*, Bruker Advanced X-ray Solutions, Bruker AXS Inc., Madison, Wisconsin, USA, 2013.
7. (a) *SHELXTL* (Version 6.14) Bruker Advanced X-ray Solutions, Bruker AXS Inc., Madison, Wisconsin, USA, 2000–2003; (b) G. M. Sheldrick, *Acta Cryst.* 2008, **A64**, 112–122.
8. G. M. Sheldrick, University of Göttingen, Germany, 2013.